Thermochimica Acta, 106 (1986) 27–34
Elsevier Science Publishers B.V., Amsterdam – Printed in The Netherlands

THE APPLICATION OF DECONVOLUTION CALORIMETRY TO THE BELOUSOV–ZHABOTINSKII REACTION

J.R. RODRIGUEZ, V. PEREZ VILLAR *, C. REY and M. GARCIA

Departamento de Termología, Facultad de Física, Universidad de Santiago de Compostela (Spain)

(Received 14 February 1986)

ABSTRACT

In the present paper we describe the determination of heat generation curves of the Belousov–Zhabotinskii reaction for various concentrations of reagents using deconvolution techniques. The experiments were carried out in a twin-vessel Calvet-type conduction calorimeter. The force of the injected jet guaranteed the initial homogeneity of the reaction mixture, and no subsequent stirring was employed. Some characteristic parameters have been calculated from the deconvoluted signal.

INTRODUCTION

In recent years considerable effort has been devoted to the study of oscillating chemical systems, in particular the Belousov–Zhabotinskii reaction [1]. Most quantitative work on this reaction has been carried out in continuous-flow, well-stirred tank reactors (CTSRs) and has sought to measure the fluctuating concentrations of the various reagents involved. Except for the work of Körös et al. [2] and Vidal and Nayau [3], relatively little research has so far been done on the associated fluctuations in the heat of reaction.

Both Körös and Vidal measured the variations in temperature of a previously calibrated vessel immersed in an isothermal shield and calculated the momentaneous heat of reaction from the temperature curve so obtained. In Vidal's case the vessel was a CTSR including a wire of negligible mass as calibrating element. Körös gives no details of the calorimeter employed. In either case, the results, though qualitatively correct, are certainly only approximate quantitatively because even if the calorimeter is assumed to be a linear system the relationship between the heat evolved in the calorimeter cell and the response signal produced by the detectors does not in general

* To whom correspondence should be addressed.

0040-6031/86/$03.50

obey Fourier's law of direct proportionality, as assumed by both of these authors. Apart from the geometry of the calorimeter, which is fixed, this relationship is affected by the heat capacity of the contents of the cell, the spatial distribution of the sources of heat, and the thermal contact between the various parts of the calorimeter [4]. In the present article we describe the determination of the heat generation curves of the Belousov–Zhabotinskii reaction for various concentrations of the reagents using rigorous data processing techniques.

EXPERIMENTAL

The experiments were carried out in a twin-vessel Calvet-type conduction calorimeter [5] each of whose cells has a capacity of 10 ml and consists of a cylinder wound with several dozen thermocouples in series. The thermopiles of the two vessels are connected in opposition so that the apparatus as a whole operates as a differential calorimeter. Above each vessel is fixed a syringe whose needle passes through the lid of the vessel into the reaction cell. The whole apparatus is housed in a system of compartments ensuring a stable environment at 25.00 °C.

The experimental cell initially contains malonic acid and bromate, and the syringe above it the catalyst (Ce(IV)) dissolved in sulphuric acid. The reference cell and its syringe both contain the stabilized (i.e. unfluctuating) products of a previous reaction using the same concentrations of reagents. This arrangement allows the viscous processes consequent upon the injection of catalyst to be compensated for. Once the apparatus is thermally stable (about 2 h after the start of the experiment), the two syringes are simultaneously discharged. The force of the injected jet guarantees the initial homogeneity of the reaction mixture, and no subsequent stirring is employed. The electromotive force generated in the thermopiles was measured using a voltmeter with a precision of 1 μV whose output was sampled by the microcomputer responsible for storing and processing the data.

THEORETICAL

A conduction calorimeter may be considered as a linear system whose response (the experimental thermogram) does not necessarily faithfully reproduce the process taking place in the calorimeter cell. Because of this, conduction calorimetry has traditionally been used to obtain integral quantities. However, by applying modern deconvolution techniques to the experimental thermograms, the actual course of the heat generation process may be reconstructed with considerable accuracy. In the localized constants model the calorimeter is represented as a set of N elements, i, with heat

capacities C_i coupled via thermal resistances R_{ij} [6]. The energy equation for element i is

$$w_i(\tau) = C_i \frac{\mathrm{d}t_i(\tau)}{\mathrm{d}(\tau)} + \sum_{\substack{j=0 \\ j \neq i}}^{N} R_{ij}\left[t_i(\tau) - t_j(\tau)\right] \qquad i = 1, 2, \ldots, N \tag{1}$$

where $t_i(\tau)$ is the temperature of element i at time τ and $w_i(\tau)$ the heat generated in this element. R_{i0} is the thermal coupling between element i and the thermostat in which the calorimeter is immersed, which is kept at the constant temperature t_0. Element 1 (the contents of the calorimeter cell) is the only one in which heat is produced, and element N houses the sensors. After expressing the temperatures t_i with respect to that of the thermostat, application of the Laplace transformation to the system of differential equations (1) yields

$$T_N(s) = H(s) W_1(s) \tag{2}$$

where $T_N(s)$ and $W_1(s)$ are, respectively, the Laplace transforms of $\theta_N(\tau) = t_N(\tau) - t_0(\tau)$ and $w_1(\tau)$, and $H(s)$, the transfer function of the calorimeter, is given by

$$H(s) = M\left[\prod_{j=1}^{N-2} (\tau_j^* s + 1) \Big/ \prod_{i=1}^{N} (\tau_i s + 1)\right] \tag{3}$$

Here τ_j^* and τ_i, the time constants of the system, and M, its sensitivity, are all functions of the heat capacities and thermal resistances of the calorimeter. A given calorimeter may be characterized, i.e. its time constants and sensitivity determined and the function $H(s)$ constructed, by studying its response to known heat inputs [7]. Conversely, once $H(s)$ is known, $w_1(\tau)$ (the power dissipated in the cell) can be found explicitly from $\theta_N(\tau)$ (the experimental thermogram) by obtaining $W_1(s)$ from eqn. (2) and applying the appropriate transformation to return to the time domain [8,9]. In the work described in this article, a five-element model was used for the calorimeter, so that $H(s)$ had five poles and three zeros.

RESULTS

Table 1 lists the initial concentrations of reagents used in the various experiments carred out. Figures 1a and 2a show representative experimental thermograms, and Figs. 1b and 2b the corresponding deconvoluted signals expressed in terms of the power dissipated in the cell per unit volume, or thermicity, given by

$$\dot{Q}_v = \frac{1}{V}\frac{\mathrm{d}Q}{\mathrm{d}\tau} = \sum_r \Delta h_r k_r \prod_j X_j^{v_{jr}} \tag{4}$$

TABLE 1

This table shows the concentrations at which oscillations have been observed. Runs labelled α and β employed, respectively sulphuric acid concentrations of 0.5 and 1 mol l^{-1}. Values of the parameters fitting eqn. (5) to the experimental thermicities are also given. T_{ind} is the duration of the induction time. A_{osc} is the area of the first peak and $\dot{Q}_t^{\infty}$ is the residual thermicity after 100 min

Run	$\alpha 1$	$\alpha 2$	$\alpha 3$	$\alpha 4$	$\alpha 5$	$\beta 1$	$\beta 2$	$\beta 3$	$\beta 4$	$\beta 5$	$\beta 6$	$\beta 7$	$\beta 8$
$[BrO_3^-]_0 \times 10^2$ (mol l^{-1})	2.5	2.5	5	10	2.5	1.5	5	2.5	5	10	1.5	5	10
$[C_3H_4O_4]_0 \times 10^2$ (mol l^{-1})	2.5	2.5	2.5	2.5	5	2.5	2.5	5	5	5	10	10	10
T_{ind} (min)	26.7	25.7	24.9	36.4	14.5	19.1	21.7	15.0	15.6	8.10	11.7	9.60	12.8
$a_0 \times 10^4$ (W cm^{-3})	5.57	7.91	6.83	8.97	8.36	7.07	12.0	11.2	18.3	22.7	5.71	22.7	42.7
$-a_1 \times 10^6$ (W $min^{-1} cm^{-3}$)	6.58	14.8	2.84	8.38	10.0	7.48	14.8	17.9	21.3	23.7	10.7	3.87	6.10
$a_2 \times 10^8$ (W $min^{-2} cm^{-3}$)	4.19	20.2	0	5.76	4.49	3.58	8.85	12.1	12.1	11.2	7.51	24.7	3.92
$A_0 \times 10^4$ (W cm^{-3})	2.23	2.69	4.92	3.72	4.47	4.63	7.80	7.53	11.0	3.55	3.34	14.4	10.7
$b \times 10^3$ (min^{-1})	1.09	2.70	1.80	2.75	0.917	2.86	3.41	4.09	4.00	3.05	3.02	3.56	4.49
T_{osc} (min)	2.76	2.68	4.15	3.20	3.00	2.61	2.18	1.64	1.50	1.19	1.55	1.11	0.714
$A_{osc} \times 10^2$ (J cm^{-3})	3.20	3.18	8.92	4.96	7.06	5.27	7.42	5.55	7.62	2.14	2.51	7.97	3.93
$\dot{Q}_t^{\infty} \times 10^4$ (W cm^{-3})	3.01	7.71	4.75	5.99	3.16	3.40	5.82	4.67	9.03	10.4	2.08	7.71	17.3

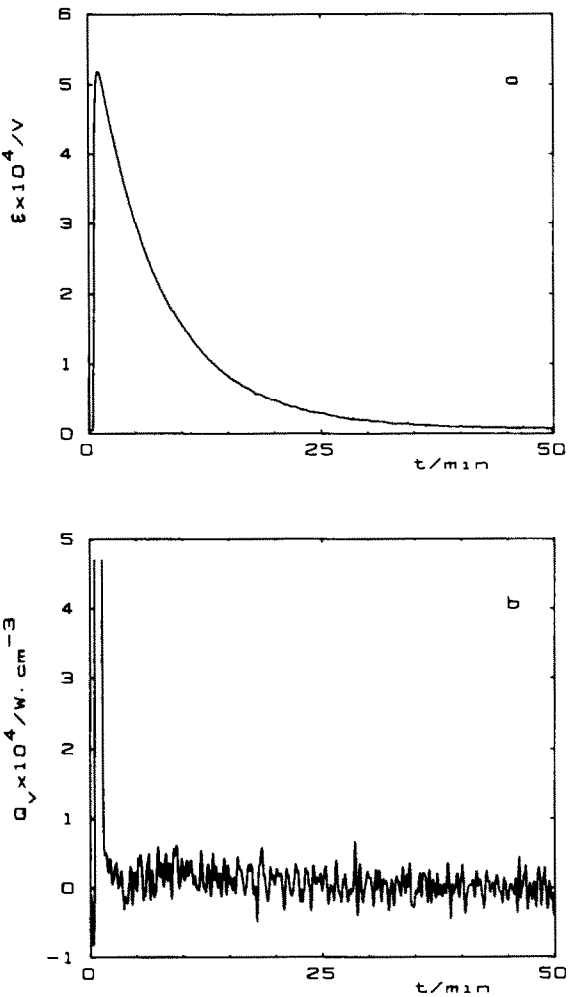

Fig. 1. A representative experiment in the non-oscillating region. The initial concentrations are $[H_2SO_4]_0 = 0.5$ M, $[Ce^4]_0 = 10^{-3}$ M, $[C_3H_4O_4]_0 = 2.5 \times 10^{-2}$ M and $[BrO_3^-]_0 = 10^{-2}$ M. (a) Experimental thermogram the shape of which is a typical pulse response of a linear system. (b) Deconvolution of (a).

where V is the volume of the reaction mixture (10 ml in all these experiments), Δh_r is the enthalpy of step r of the reaction mechanism, k_r is the rate constant of step r, X_j the concentration of chemical species 1 and ν_{jr} the stoichiometric coefficient of species j in step r.

The curves of Fig. 1 correspond to the concentration at which no oscillation occurs. The sharp peak near the origin, which represents the heat liberated during the initial mixing process, is followed by a fuzzy band about zero which, in the case of Fig. 1b, represents both instrumental and numerical noise associated with the deconvolution process [9,10]. The mean (10^{-5} W cm^{-3}) and root mean square (4×10^{-10} W cm^{-6}) of this band

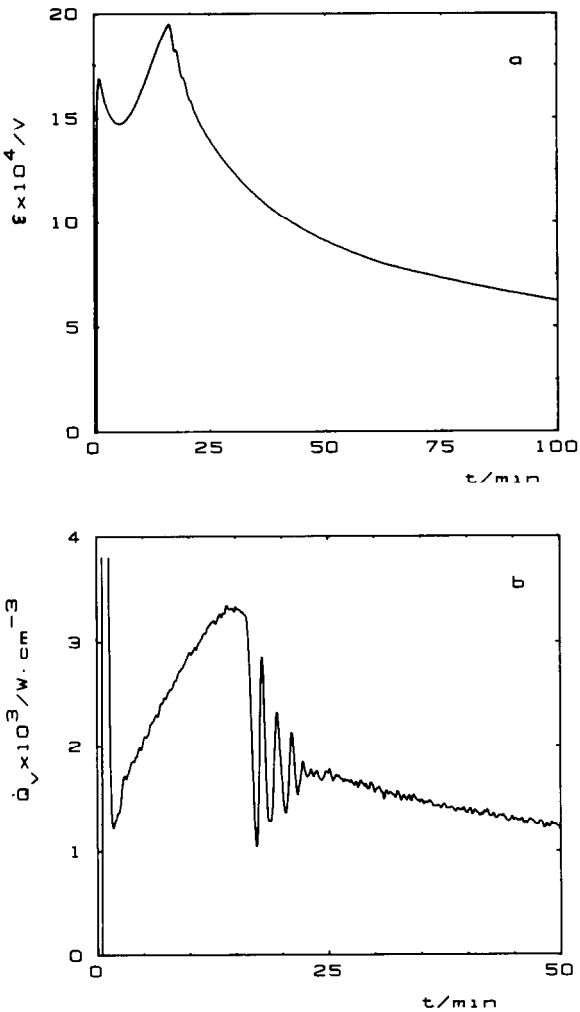

Fig. 2. A representative experiment in the oscillatory region, corresponding to run $\alpha 3$ of Table 1. (a) Experimental thermogram, (b) its deconvolution. After the induction time, several oscillations are present whose damping is perhaps due to the lack of stirring.

characterize the noise and enable it to be distinguished from oscillation due to the reaction itself in other experiments.

In Fig. 2a, which is a typical thermogram of oscillating reactions [11], the initial sharp peak is followed by another, the relative heights of the two depending on the concentrations of malonic acid and bromate ions (raising the concentration of sulphuric acid merely raises the level of the thermogram). The time taken to increase to the second peak (induction time) is listed in Table 1 for each of the experiments carried out. It is the fall from this peak that produces the onset of oscillations, which in the present

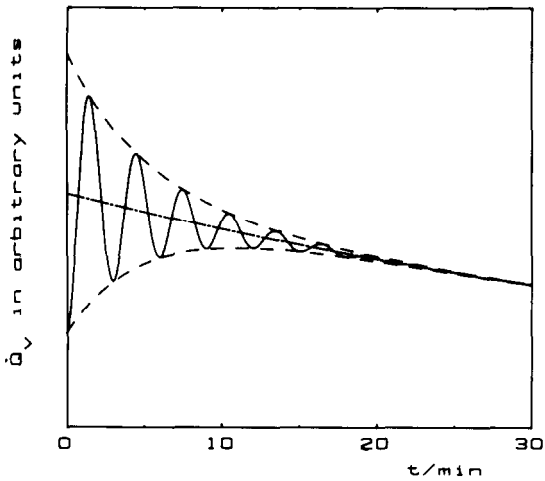

Fig. 3. General shape of the curve fitted to the oscillations and subsequent tails of the thermicities $\dot{Q}_v$.

experiment number from three to six. After the oscillations have died away the residual thermicity slowly decays to zero.

In order to obtain a functional model of the processes from the approach to oscillation onwards, the initial peak and the induction period were suppressed from the deconvoluted curves and a function of the form

$$\dot{Q}_v = a_0 + a_1\tau + a_2\tau^2 - A_0\, e^{-bt} \cos 2\pi \frac{\tau}{T_{osc}} \tag{5}$$

fitted to the remainder up to 100 min after initiation of the reaction. Equation (5) represents a damped oscillation (the final term on the right-hand side) superimposed on a quadratic decay process (the first three terms). A typical curve of this type is shown in Fig. 3. The parameters a_0, a_1, a_2, A_0, b and T_{osc} have been calculated from the deconvoluted signal for each experiment exhibiting oscillation by a conventional non-linear regression algorithm [12]. The area of the first oscillation (Fig. 3) and the residual thermicity after 100 min, both calculated from the fitted curve, are listed for each experiment in Table 1.

CONCLUSIONS

The concentrations at which oscillation occurred in these experiments agree with the findings of other authors [12]. The oscillatory region of the heat generation curves may be treated as a damped oscillation superimposed on a monotonic decay. The natural frequency of the oscillations has been calculated for the experimental conditions used (a closed vessel lacking any

kind of thermometer, electrode or other detecting element in its interior that might affect the course of the reaction).

The low number of oscillations observed in the present experiments may be due to not having employed any kind of stirring, which obviously allowed diffusion processes to take place. These may have resulted in the phase of the reaction varying from one part of the reaction chamber to another, and the different contributions to the overall heat signal cancelling each other out.

REFERENCES

1 For a general review, see, for example: G. Nicolis and J. Portnow, J. Chem. Rev., 73 (1973) 365; A. Pascault and C. Vidal, J. Chim. Phys., 79 (1982) 691.
2 E. Körös, M. Orban and Zs. Nagy, J. Phys. Chem., 67 (1973) 3122.
3 C. Vidal and A. Nayau, J. Am. Chem. Soc., 102 (1980) 6666.
4 C. Rey, Ph.D. Thesis, University of Santiago de Compostela, 1983.
5 E. Calvet and H. Prat, Microcalorimeter, Massons, Paris, 1956.
6 J. Navarro, E. Cesari, V. Torra, J.L. Macqueron, J.P. Dubes and H. Tachoire, Thermochim. Acta, 52 (1982) 175, 193.
7 J.R. Rodríguez, C. Rey, V. Pérez-Villar, J.P. Dubes, H. Tachoire and V. Torra, Thermochim. Acta, 75 (1984) 51, 58.
8 C. Rey, J.R. Rodríguez and V. Pérez Villar, Thermochim. Acta, 61 (1984) 1, 11.
9 J.R. Rodríguez, C. Rey, V. Pérez Villar, V. Torra, J. Ortín and J. Viñals, Thermochim. Acta, 63 (1983) 331, 339.
10 V. Pérez Villar, C. Rey and J.R. Rodríguez, Thermochim. Acta, 79 (1984) 111, 116.
11 W. Geiseler and K. Bar-Eli, in K.H. Ebert, P. Deuflhard and W. Jäger (Eds.), Modelling of Chemical Reaction Systems, Springer-Verlag, Berlin, 1981.
12 P.R. Bevington, Data Reduction and Error Analysis for the Physcial Sciences, McGraw-Hill, New York, 1969.